

STUDY ON THE ONSET CONDITION AND TRANSIENT BEHAVIORS OF NOISE-INDUCED BIFURCATION

Zigang Li

State Key Laboratory for Strength and Vibration
Xi'an Jiaotong University
China
lzghsfy@hotmail.com

Kongming Guo

School of Electromechanical Engineering
Xidian University
China
kmguo@xidian.edu.cn

Jun Jiang

State Key Laboratory for Strength and Vibration
Xi'an Jiaotong University
China
jun.jiang@mail.xjtu.edu.cn

Ling Hong

State Key Laboratory for Strength and Vibration
Xi'an Jiaotong University
China
hongling@xjtu.edu.cn

Abstract

To efficiently determine critical condition of noise-induced bifurcation in nonlinear dynamical systems, a stochastic sensitivity function (SSF) around a deterministic periodic attractor is approximated based on stroboscopic mapping. In this way, the confidence ellipses are constructed to judge critical noise intensity of noise-induced transition phenomena. To effectively capture the larger stochastic transient behaviors after the critical condition, an idea of evolving probabilistic vector (EPV) is introduced into the Generalized Cell Mapping method (GCM) in order to enhance the computation efficiency of the numerical method. The feasibility of the two proposed methods is demonstrated through the study of a pendulum system under external periodic excitation and additive noise.

Key words

Stochastic sensitivity function, stroboscopic map, generalized cell mapping, evolving probabilistic vector, noise-induced transition.

1 Introduction

Noise is ubiquitous in nature and engineering systems that are all inherently nonlinear. Uncertain disturbances or noises on nonlinear dynamical systems often evoke some unexpected and even coherent responses. Various noise-induced behaviors have been found, such as noise-induced chaos [Zhang, Tabata, Tsuchiya, 2011; Tel and Lai, 2010], stochastic bifurcation [Malick and Marcq, 2003; Xu, He, Fang, 2003], noise-induced intermittency [Kraut and Feudel, 2003], noise-induced hopping [Arecchi, Badii and Politi, 1985; Kraut and

Feudel, 2002] and so on.

In [Thompson, Stewart, and Udea, 1994], the bifurcations of deterministic (dissipative) nonlinear dynamical systems are classified into three categories: safe, explosive and dangerous. The explosive bifurcations are defined as catastrophic global bifurcations with an abrupt enlargement of the attracting set but with no jump to remote disconnected attractor. The dangerous bifurcations are catastrophic bifurcations with blue-sky disappearance of the attractor with a sudden fast jump to a distant unrelated attractor. Undoubtedly, these two kinds of bifurcations have very important engineering meaning since they imply that abrupt and great change in the operation state of a machine or a system takes place with a continuous variation of a parameter that may even induce possible damage or destruction of the system. Since uncertain disturbance is usually unavoidable in real engineering environment, it is thus of great interest to exploit the quantitative prediction on responses of periodic attractors under noise excitation, and how to capture the transient responses of the noise-induced large transition when such bifurcation occurs. They are the two purposes of the present paper.

It is well known that Monte-Carlo simulation (MCS) is a direct method to obtain the probabilistic distribution of a stochastic system, but it is too expensive in computations to be used for a systematic investigation. For the case of excitation under Gaussian white noise, the probabilistic description of the stochastic responses is governed by Fokker-Planck-Kolmogorov (FPK). Several approximate methods on solving FPK equation have been developed, including Finite Element Method [Spencer and Bergman, 1993], exponential-polynomial closure method [Zhu, 2012],

stochastic averaging procedure [Gu and Zhu, 2014], path integral method [Wehner and Wolfer, 1983; Di Paola and Santoro, 2009], etc.

Based on the quasi-potential theory, the stochastic sensitivity function, proposed by Bashkirtseva, can give an approximate analytical description of the probabilistic distribution. This method is easier than other FPK equation-based methods and has successfully applied to analysis the sensitivity of stationary point, 2D cycle, 3D cycle in differential dynamical systems. For discrete systems, the sensitivity of fixed point and periodic solution can also be analyzed using SSF [Bashkirtseva, Ryashko, and Tsvetkov, 2010]. Moreover, SSF can help to stabilize the equilibrium in noise disturbed chaotic system [Bashkirtseva, Chen, and Ryashko, 2012]. In this paper, a non-autonomous dynamical system is discretized into a discrete map by $1/N$ -period stroboscopic map. Through solving stochastic sensitivity functions of periodic attractors in maps, confidence ellipses were constructed to describe the distributions of the random attractors. In this way, boundary value problems of matrix differential equations were avoided, while there were and only matrix algebra equations need to be solved. Thus, probabilistic distribution of periodic attractors can be analytically predicted when the explosive bifurcation occurs.

Generalized Cell Mapping method, which was pioneered by Hsu [Xsu, 1981; Xsu, 1987] in 1980s, may effectively deal with the global analysis of stochastic dynamic systems [Sun and Hsu, 1988] and capture noise-induced probability evolution for a invariant sets to another, especially for the dangerous bifurcations. But, like many other numerical methods for stochastic dynamics, the computational efficiency is still a crucial problem faced by GCM that needs to be solved with effort. In the study, we are interest in the probability distribution of the initial states localizes near a given deterministic attracting set. Thus, the traditional GCM that always deals with a priori defined sufficient large chosen region in the state space is not quite efficient for the analysis of the above problem. Therefore, the idea of evolving probabilistic vector (EPV) is introduced in this paper in order to enhance the efficiency of the GCM. By using EPV, only the one-step transition probability of the cells in the chosen region, whose probabilities are within a given fiducial probability, will be calculated, instead of all the cells within the chosen region in the state space. In this way, the dimension of the probabilistic vector in the present GCM method (GCM with EPV), which varies with the evolution of the stochastic response, is greatly reduced and usually much smaller than that of the corresponding fix-sized probabilistic vector. This paper is organized as follows: In Section 2, the algorithm to obtain SSF of periodic attractors in non-autonomous nonlinear system is proposed by constructing $1/N$ -period stroboscopic map. Section 3, the idea of evolving probabilistic vector is proposed in order to enhance the efficiency of the GCM, and the corresponding algorithm is devised. In

Section 4, the proposed methods are applied to a pendulum system under external periodic excitation and additive noise. Finally, conclusions are drawn in Section 5.

2 Stochastic Sensitivity Function of Periodic Attractors

Consider a continuous non-autonomous dynamical system

$$\dot{\mathbf{x}} = \mathbf{f}(\mathbf{x}, t) \quad (1)$$

where \mathbf{x} is n -dimensional non-autonomous vector field depending on both state \mathbf{x} and time t .

When there is a periodic attractor with period T in non-autonomous system (Eq. 1), a stroboscopic map at discrete times $t = t_0 + k\Delta t$ (k is positive integer) is often used to investigate the character of the attractor, which can be defined as

$$\mathbf{x}_{k+1} = \varphi_{\Delta t}(\mathbf{x}_k) \quad (2)$$

However, though the algorithm to get SSF of fixed point of maps is raised in [Bashkirtseva, Chen, and Ryashko, 2012], for most of the nonlinear dynamical systems, the explicit expression of 1-period stroboscopic map cannot be obtained.

Note that, if $\Delta t \rightarrow 0$, the linear approximation of map Eq. 2 can be taken in the interval $[t_0 + k\Delta t, t_0 + (k+1)\Delta t]$

$$\mathbf{x}_{k+1} = \exp(\mathbf{J}_k \Delta t) \mathbf{x}_k \quad (3)$$

where $\mathbf{J}_k = \frac{\partial \mathbf{f}}{\partial \mathbf{x}} \big|_{\mathbf{x}=\mathbf{x}_k, t=t_0+k\Delta t}$ is Jacobian matrix at point \mathbf{x}_k and time $t_0 + k\Delta t$.

So, the sampling time interval Δt of stroboscopic map can be set to

$$\Delta t = T/N, \quad N \gg 1 \quad (4)$$

and a new stroboscopic map can be written in the form Eq. 3. This new map is named as a $1/N$ -period stroboscopic map.

Through this new map, the original periodic attractor Γ is discretized into a period- N cycle $\Gamma^* = \{x_1, \dots, x_N\}$ by N stroboscopic sections $\{\Sigma_1, \dots, \Sigma_N\}$. (see Fig. 1)

Now consider system Eq. 1 subject to stochastic disturbance

$$\dot{\mathbf{x}} = \mathbf{f}(\mathbf{x}, t) + \varepsilon \sigma(\mathbf{x}) \xi(t) \quad (5)$$

where ξ is n -dimensional Gaussian white noise, σ is $n \times n$ matrix which defines the relation between the noise and the system state, ε is the noise intensity.

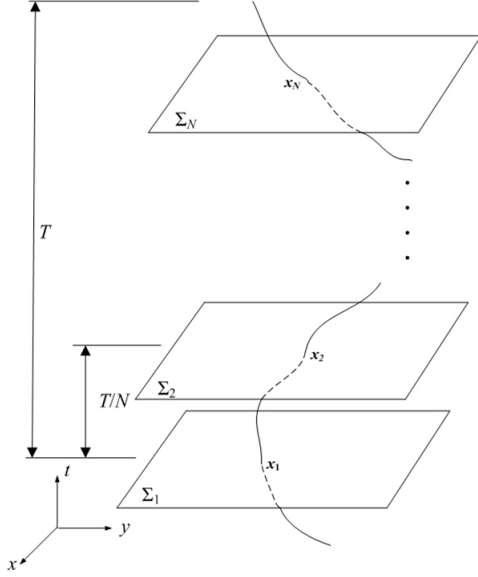


Figure 1. $1/N$ -period stroboscopic map of a 2-dimensional non-autonomous system.

The $1/N$ -period stroboscopic map of system is written as

$$\mathbf{x}_{k+1} = \exp(\mathbf{J}_k \Delta t) \mathbf{x}_k + \varepsilon \sigma(\mathbf{x}_k) \Delta \mathbf{w} \quad (6)$$

where

$$\Delta \mathbf{w} = \sqrt{\Delta t} \xi$$

is an increment of Wiener process during time interval $[t_0 + k\Delta t, t_0 + (k+1)\Delta t]$.

According to [Bashkirtseva, Ryashko, and Tsvetkov, 2010], if the deterministic period- N cycle in Eq. 3 is exponentially stable in its neighborhood, one can define

$$\left. \begin{aligned} \mathbf{S}_k &= \sigma(\mathbf{x}_k), \mathbf{Q}_k = \mathbf{S}_k \mathbf{S}_k^T, \mathbf{F}_k = \exp(\mathbf{J}_k \Delta t) \\ k &= 1, \dots, N \\ \mathbf{B} &= \mathbf{F}_N \mathbf{F}_{N-1} \dots \mathbf{F}_2 \mathbf{F}_1 \\ \mathbf{Q} &= \mathbf{Q}_N + \mathbf{F}_N \mathbf{Q}_{N-1} \mathbf{F}_N^T + \mathbf{F}_N \mathbf{F}_{N-1} \mathbf{Q}_{N-1} \mathbf{F}_{N-1}^T \mathbf{F}_N^T \\ &+ \dots + \mathbf{F}_N \dots \mathbf{F}_2 \mathbf{Q}_1 \mathbf{F}_2^T \dots \mathbf{F}_N^T \end{aligned} \right\} \quad (7)$$

If the period- N cycle is attractor, it is always exponentially stable. The SSF of point \mathbf{x}_1 is then the unique solution of matrix equation

$$\mathbf{W}_1 = \mathbf{B} \mathbf{W}_1 \mathbf{B}^T + \mathbf{Q} \quad (8)$$

and $\mathbf{W}_2, \mathbf{W}_3, \dots, \mathbf{W}_N$ can then be calculated by the recurrence relation blow

$$\mathbf{W}_{k+1} = \mathbf{F}_k \mathbf{W}_k \mathbf{F}_k^T + \mathbf{Q}_k, \quad k = 1, \dots, N-1 \quad (9)$$

After \mathbf{W}_k is calculated, a confidence ellipse that represents the spatial distribution of stochastic states concentrated near point \mathbf{x}_k in stroboscopic section Σ_k can

be obtained using the following equation:

$$(\mathbf{x} - \mathbf{x}_k)^T \mathbf{W}_k^{-1} (\mathbf{x} - \mathbf{x}_k) = 2\varepsilon^2 \Delta t (-\ln(1-P)) \quad (10)$$

where $P \approx 1$ is the fiducial probability, with which the points in the stochastic attractor are contained in the ellipse.

3 GCM with Evolving Probabilistic Vector

In this part, GCM with evolving probabilistic vector will be developed to capture large stochastic transition of a nonlinear system under noise.

The response of a N -dimensional nonlinear system subjected to additive and/or multiplicative Gaussian white noise excitations is well known to be a diffusion Markov process. Based on the Generalized Cell Mapping method, the probability evolution of the stochastic system is described by a homogeneous Markov chain in the cell space as

$$\mathbf{P} \cdot \mathbf{p}(n) = \mathbf{p}(n+1) \quad (11)$$

where $\mathbf{p}(n)$ denotes the probabilistic vector describing the probability of each cell at n th step, and \mathbf{P} the one-step transition probability matrix of the stochastic system. The element P_{ij} and $p_i(n)$ can be determined by following formulae

$$\left. \begin{aligned} P_{ij} &= \int_{C_i} p(\mathbf{x}, t | \mathbf{x}_j, t_0) d\mathbf{x} = \int_{C_i} p(\mathbf{x}, \tau | \mathbf{x}_j, t_0) d\mathbf{x} \\ p_i(n) &= \int_{C_i} p(\mathbf{x}, n\tau) d\mathbf{x} \end{aligned} \right\} \quad (12)$$

where $\tau = t - t_0$ denotes a mapping time step; C_i is the domain occupied by i th cell in \mathbf{R}^N , and $p(\mathbf{x}, \tau | \mathbf{x}_j, t_0)$ and $p(\mathbf{x}, n\tau)$ represent the one-step transition probability and the probability under n -steps mapping in \mathbf{R}^N , respectively.

A Gauss-Legendre quadrature is applicable to estimate the above integral in domain C_i . This means that probabilities in i th cell are discretely expressed by that at Gauss quadrature points in the cell. Therefore, based on this rule

$$\left. \begin{aligned} P_{ij} &= \sum_{k=1}^{S_i} A_k p(\mathbf{x}^k, \tau | \mathbf{x}_j, t_0), \\ p_i(n) &= \sum_{k=1}^{S_i} A_k p(\mathbf{x}^k, n\tau) \end{aligned} \right\} \quad (13)$$

where \mathbf{x}_j is the geometrical center of j th cell; \mathbf{x}^k is the k th Gauss quadrature point, S_i is the number of Gauss quadrature points in i th cell, and A_k is the quadrature factor.

To release the difficulty of huge time-consumption in solving nonlinear stochastic equations based on sampling methods, like straightforward MCS to estimate the one-step transition probability matrix P_{ij} , a short-time Gaussian approximation approach proposed in [Sun and Hsu, 1990] is adopted. The distribution can

be approximately specified by the mean and the variance. can be evaluated by integrating moment equations from $t=0$ to $t=\tau$.

Borrowing the idea from Point Mapping under Cell Reference method [Jiang, 2011; Jiang, 2012], the cells in the chosen region will be classified into active cells and inactive cells. An *active cell* represents the cell whose probability density function (PDF) is within the prescribed fiducial probability, and an *inactive cell* is the cell whose PDF is outside the prescribed fiducial probability, as shown in Fig. 2. In simulation, the inactive cells can be neglected in the computation of the short-time mapping, that is, $P_{ir}p_r=0$ when r th cell is an inactive cell.

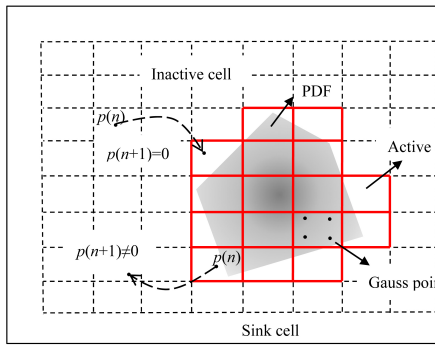


Figure 2. Schematic representations of fiducial probability and active cell, inactive cell, sink cell.

So the probabilistic vector $\mathbf{p}(n)$ in the present work is no longer a vector with a fixed length N as in the traditional GCM, rather its length will vary and equal the number of active cells. Then the evolving probabilistic vector is governed by

$$\begin{cases} P_{ij}p_j(n) = 0 & j = r \\ P_{ij}p_j(n) = p_i(n+1) & j \neq r \end{cases} \quad j = 1, 2, 3, \dots, N \quad (14)$$

4 Stochastic Responses in Noise-induced Duffing Oscillator

To demonstrate the capability of above proposed methods, a pendulum system under external periodic excitation and additive noise

$$\ddot{\theta} + c\dot{\theta} + \sin(\theta) = B\cos(t) + \sigma_w w(t) \quad (15)$$

where $w(t)$ a Gaussian white noise stochastic process as defined as

$$\left. \begin{aligned} E[w(t)] &= 0 \\ E[w(t)w(t+\tau)] &= \delta(\tau) \end{aligned} \right\} \quad (16)$$

where σ_w is the noise intensity. Let us fix the parameters $c=0.2$ and $B=2.0$. For the deterministic case, namely $\sigma_w=0$, two period-1 attractors coexist, corresponding respectively to the clockwise (θ^-) and counterclockwise (θ^+) periodic rotation of the variable θ_1 . Two chaotic saddles are included in each basin of attraction, and a chaotic saddle on boundaries of basins of attraction is detected and shown in Fig. 3.

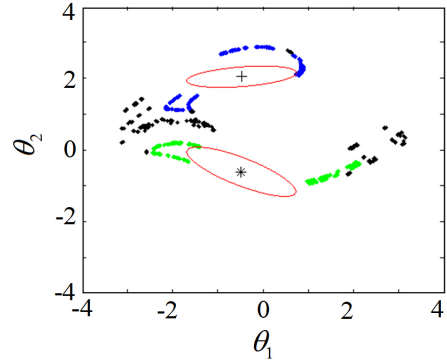


Figure 3. Global dynamical structure of pendulum system when $c=0.2$, $B=2.0$, $\sigma_w=0.0$, +represents attractor of θ^+ and *stands for attractor of θ^- . The chaotic saddle in the basin of θ^+ is marked by blue and in the basin of θ^- by green. The chaotic saddle on basin boundaries is depicted in black. The red curves stands for confidence ellipses with critical noise intensities.

4.1 Sensitivity Analysis

It is not hard to imagine that the stochastic responses will respectively concentrate, depending upon initial condition, around the deterministic attractors when the noise intensity is sufficient small. The method proposed in Section 2 is employed to investigate the confidence ellipse of the two attractors. Let $N=300$, $\Delta t = T/N = 0.02\pi$ and the fiducial probability $P=99\%$. By increasing the noise intensity, the size of confidence ellipses increases. When $\sigma_w=0.077$ the ellipses begin to touch the chaotic saddle in the basin of (θ^+), while $\sigma_w=0.089$ for the clockwise (θ^-) periodic rotation (see Fig. 3). To check our prediction, let us first take noise intensity $\sigma_w=0.03$, and MCS are used to show its validity. The confidence ellipse is found to be in very good agreement with MCS results (see Fig. 4).

However, when noise intensities are up to the critical, say to $\sigma_w=0.077$ for the case of initial counterclockwise rotation (Fig. 5a) or $\sigma_w=0.089$ for the case of initial clockwise rotation (Fig. 5b), noise-induced bifurcation occurs that most of response realizations are still concentrated around the initial attractor, but a portion of the response realizations go around the another attractor. Now, the quantification of the probabilistic distribution of noise-induced bifurcation can not be well predicted by the stochastic sensitivity function technique.

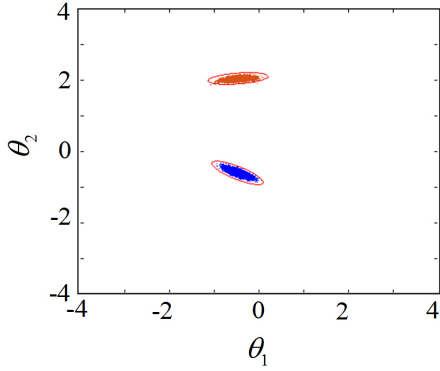


Figure 4. The confidence ellipses predicted by SSF when noise intensity $\sigma_w=0.03$: red dots is for the initial counterclockwise rotation; blue dots for the initial clockwise rotation.

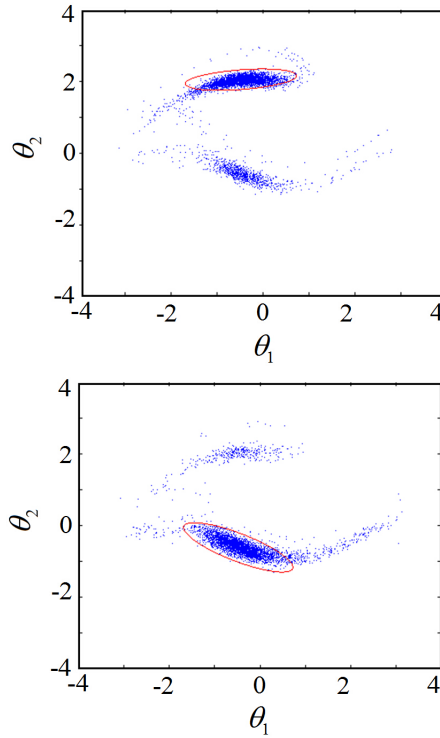


Figure 5. The confidence ellipses predicted by SSF: (a) noise intensity $\sigma_w=0.077$ for the initial counterclockwise rotation; (b) noise intensity $\sigma_w=0.089$ for the initial clockwise rotation.

4.2 Noise-induced Transition

Recalling the stochastic equation defined in 15, Let $m_{pq} = E[\theta^p \dot{\theta}^q]$, a set of moment evolution equations are derived by applying Gaussian closure to using the

short-time Gaussian approximation approach

$$\left. \begin{aligned} \dot{m}_{10} &= m_{01} \\ \dot{m}_{01} &= -cm_{01} - E[\sin(\theta_1)] + B\cos(t) \\ \dot{m}_{20} &= 2m_{11} \\ \dot{m}_{11} &= m_{02} - cm_{11} - E[\sin(\theta_1) \cdot \theta_1] + \\ &\quad B\cos(t) \cdot m_{10} \\ \dot{m}_{02} &= -cm_{02} - E[\sin(\theta_1) \cdot \theta_2] + \\ &\quad B\cos(t) \cdot m_{02} + \sigma_w^2 \end{aligned} \right\} \quad (17)$$

It should be noted that several expected values in these equations cannot be analytically expressed by lower order moments. Thus, these non-analytically closeable functions in Eq. 17 are approximated by second-order Taylor expansions about the cell centers [Sun and Hsu, 1990].

In this part, we are interested in noise-induced transition responses. By using the proposed GCM with EPV, the chosen domain of x and \dot{x} is taken to be $[1.5, 4.2] \times [-3.0, 6.0]$, and covered by 500×500 cells with 0.0054×0.018 resolution on the chose region. In the subsequent discussion, we will only discuss the case that the initial conditions is clockwise rotation that locate on the basin of (θ_-) and the chaotic saddle in the basin, similar phenomena can be predicted for the counterclockwise case.

Fig. 6 shows that response PDF corresponding to noise-induced transition is more accurately illustrated contrasting with Fig. 5b.

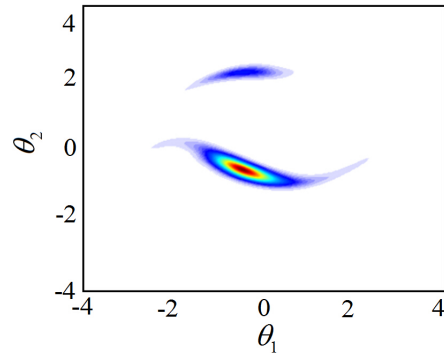


Figure 6. The stable-state PDFs predicted by GCM-EPV when noise intensity $\sigma_w=0.089$ from initial PDF around $(-0.479453, -0.609005)$.

It is interesting to note that when $\sigma_w=0.05$, the probability transition induced by noisy have not occurred in the parameters, namely no qualitative change takes place on the stochastic responses around two attractors. But, It is found from the Fig. 7 that a portion of response realizations evolve from the initial condition at point $(-1.91498174, -0.21192607)$ that locate on the chaotic saddle in the basin of (θ_-) to the remote disconnected attractor (θ_+) . Finally, the stable-state PDF

is distributed around these two attractors. It can be explained that as the increase of noise intensity, among the two chaotic saddles in different basins of attraction and a chaotic saddle on boundaries of basins of attraction start to enlarge, and when $\sigma_w=0.05$ they collide and merge into a new chaotic saddle on the boundaries covering the places of the original three chaotic saddles. Then, the global characteristic of the stochastic pendulum system have been transformed into a new structure, that is two attractors and a chaotic saddles on the boundaries of basin of attraction.

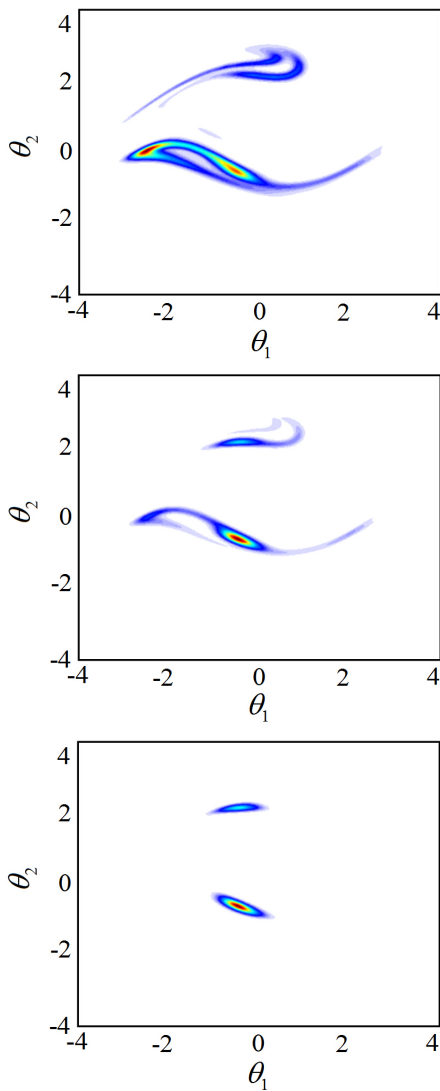


Figure 7. The transient PDFs predicted by GCM-EPV when noise intensity $\sigma_w=0.05$ from initial PDF around $(-1.91498174, -0.21192607)$: (a) at $t=6T$; (b) at $t=10T$; (c) at $t=100T$.

When the noise intensity is increased, say to $\sigma_w=0.16$, the stable-state PDF of the stochastic response will fill into a region covering both the two attractors gradually to form a stochastic new attractor as shown by Fig. 8. The stochastic responses increases the response region

abruptly through the connection of the two attractors and the chaotic saddle on the boundaries of basin of attraction, which is defined as a noise-induced explosive bifurcation [Thompson, Stewart, and Udea, 1994].

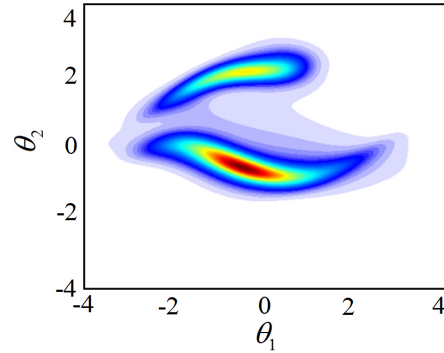


Figure 8. The stable-state PDFs predicted by GCM-EPV when noise intensity $\sigma_w=0.16$ from initial PDF around $(-0.479453, -0.609005)$.

5 Conclusions

To efficiently capture critical condition of periodic attractors in noise-induced nonlinear dynamical systems, the sensitivity of the periodic attractors is analyzed by discretize the non-autonomous system into a discrete $1/N$ -period stroboscopic map. In order to obtain the critical noise intensity of noise-induced transition phenomena, SSF is used to judge if the corresponding confidence ellipse is in touch with certain saddle-typed invariant sets. In this way, boundary value problems of matrix differential equations were avoided by solving only matrix algebra equations. SSF can give an approximate analytical description of the distribution, while its implementation is easy. The effectiveness of this method is verified by comparing the confidence ellipses with the stochastic attractors through the Monte Carlo simulation. To validity investigate the larger stochastic transition and bifurcation of nonlinear dynamical systems after the critical condition, an idea of evolving probabilistic vector is introduced into the Generalized Cell Mapping method to enhance the computation efficiency of the numerical method. By using EPV, both computation consumption and memory storage are much more reduced to make the method even more suitable for detection of large stochastic transition in stochastic systems. Final, a pendulum system under external periodic excitation and additive noise is studied as an example of application.

Acknowledgements

This work was supported by the National Natural Science Foundation of China under Grant No. 11332008 (Key Project) as well as 11172223 and 11172224.

References

- Arecchi, F.T., Badii, R., Politi, A. (1985). Generalized multistability and noise-induced jumps in a nonlinear dynamical system. *Phys. Rev. A* **32**, pp. 402–408.
- Bashkirtseva, I.A., Chen, G.R., Ryashko, L.B. (2012). Stochastic equilibria control and chaos suppression for 3D systems via stochastic sensitivity synthesis. *Commun. Nonlinear Sci. Numer. Simul.* **17**, pp. 3381–3389.
- Bashkirtseva, I.A., Chen, L.B., Tsvetkov, I.N. (2010). Sensitivity analysis of stochastic equilibria and cycles for the discrete dynamic systems. *Dynam. Cont. Dis. Ser. A* **17**, pp. 501–515.
- Di Paola, M., Santoro, R. (2009). Path integral solution handled by Fast Gauss Transform. *Probab. Engng. Mech.* **24**, pp. 300–311.
- Gu, X.D., Zhu, W.Q. (2014). A stochastic averaging method for analyzing vibro-impact systems under Gaussian white noise excitations. *J. Sound Vib.* **33**, pp. 2632–2642.
- Xsu, C.S. (1981). A generalized theory of cell-to-cell mapping for nonlinear dynamical systems. *J. Appl. Mech.* **48**, pp. 634–642.
- Xsu, C.S. (1981) *Cell to Cell Mapping: A method of global analysis for nonlinear systems*. Springer-Verlag. Germany.
- Jiang, J. (2011). A two scaled numerical method for global analysis of high dimensional nonlinear systems. *Theor. Appl. Mech. Lett.* **1**, Article ID 063001.
- Jiang, J. (2012). An effective numerical procedure to determine saddle-type unstable invariant limit sets in nonlinear systems. *Chinese Phys. Lett.* **29**, Article ID 050503.
- Kraut, S., Feudel, U. (2002). Multistability, noise, and attractor hopping: The crucial role of chaotic saddles. *Phys. Rev. E* **66**, pp. 1–4.
- Kraut, S., Feudel, U. (2002). Noise-induced escape through a chaotic saddle: lowering of the activation energy. *Physica D* **181**, pp. 222–234.
- Li, Z.G., Jiang, L.B., Hong, L. (2010). Transient behaviors in noise-induced bifurcations capture by Generalized Cell Mapping method with evolving probabilistic vector. *Int. J. Bifurcat. Chaos* **25**, pp. 1550109.
- Malick, K., Marcq, P.C. (2003) Stability analysis of a noise-induced Hopf bifurcation. *Eur. Phys. J. D.* **36**, pp. 119–128.
- Roy, R.V. (1995). Noise-induced transitions in weakly nonlinear oscillators near resonance. *J. Appl. Mech.* **62**, pp. 496–504.
- Spencer, B.F., Bergman, L.A. (1993). On the numerical solutions of the Fokker-Planck equations for nonlinear stochastic systems. *Nonlinear Dynam.* **4**, pp. 357–372.
- Sun, B.F., Hsu, C.S. (1988). A statistical study of generalized cell mapping. *J. Appl. Mech.* **55**, pp. 694–701.
- Sun, B.F., Hsu, C.S. (1990). The Generalized cell mapping method in nonlinear random vibration based upon short-time Gaussian approximation. *J. Appl. Mech.* **57**, pp. 1018–1025.
- Tel, T., Lai, Y.C. (2010). Quasipotential approach to critical scaling in noise-induced chaos. *Phys. Rev. E* **81**, pp. 1–8.
- Thompson, J.M.T., Stewart, H.B., Ueda, Y. (1994). Safe, explosive and dangerous bifurcation in dissipative dynamical system. *Commun. Phys. Rev. E* **49**, pp. 1019–1027.
- Wehner, B.F., Wolfer, W.G. (1983). Numerical evaluation of path-integral solutions to Fokker-Planck equations. *Phys. Rev. A* **27**, pp. 2663–2670.
- Xu, W., He, Q., Fang, T, et al. (2003). Global analysis of stochastic bifurcation in Duffing system. *Int. J. Bifurcat. Chaos* **13**, pp. 3115–3123.
- Zhang, W.M., Tabata, O., Tsuchiya, T, et al. (2011). Noise-induced chaos in the electro-statically actuated MEMS resonators. *Phys. Lett. A* **23**, pp. 2903–2910.
- Zhu, H.T. (2012). Probabilistic solution of some multi-degree-of-freedom nonlinear systems under external independent Poisson white noises. *J. Acoust. Soc. Am.* **131**, pp. 4550–4557.